The Astrophysical Journal, 795:88 (7pp), 2014 November 1 doi:10.1088/0004-637X/795/1/88

FERMI VARIABILITY STUDY OF THE CANDIDATE PULSAR BINARY 2FGL J0523.3−2530

Yi Xing[1], Zhongxiang Wang[1], and C.-Y. Ng[2]
[1] Shanghai Astronomical Observatory, Chinese Academy of Sciences, 80 Nandan Road, Shanghai 200030, China
[2] Department of Physics, The University of Hong Kong, Pokfulam Road, Hong Kong
Received 2014 July 7; accepted 2014 September 12; published 2014 October 15

ABSTRACT

The *Fermi* source 2FGL J0523.3−2530 has recently been identified as a candidate millisecond pulsar binary with an orbital period of 16.5 hr. We have carried out detailed studies of the source's emission properties by analyzing data taken with the *Fermi* Large Area Telescope in the 0.2–300 GeV energy range. Long-term, yearly variability from the source has been found, with a factor of four flux variations in 1–300 GeV. From spectral analysis, we find an extra spectral component at 2–3 GeV that causes the source brightening. While no orbital modulations have been found from the *Fermi* data over the whole period of 2008–2014, orbital modulation in the source's >2 GeV emission is detected during the last 1.5 yr of the *Fermi* observation. Our results support the millisecond pulsar binary nature of 2FGL J0523.3−2530. Multi-wavelength observations of the source are warranted in order to find any correlated flux variations and thus help determine the origin of the long-term variability, which currently is not understood.

Key words: binaries: close – stars: individual (2FGL J0523.3, 2530) – stars: low-mass – stars: neutron

Online-only material: color figures

1. INTRODUCTION

Since the *Fermi Gamma-ray Space Telescope* was launched in 2008 June, the main instrument on board, the Large Area Telescope (LAT), has been continuously scanning the whole sky every three hours in the energy range from 20 MeV to 300 GeV, discovering and monitoring γ-ray sources with much improved spatial resolution and sensitivity compared to older γ-ray telescopes (Atwood et al. 2009). In 2012, using *Fermi*/LAT data from the first two-year survey, a catalog of 1873 γ-ray sources was released by Nolan et al. (2012) as the *Fermi*/LAT second source catalog (2FGL). Among the γ-ray sources, 575 of them are not associated with any known astrophysical objects (Nolan et al. 2012). For the purpose of identifying the nature of these unassociated sources, many follow-up studies, such as classifying their γ-ray characteristics (Ackermann et al. 2012), searching for radio pulsars (Ray et al. 2012), and observing at multi-wavelengths (Takeuchi et al. 2013; Acero et al. 2013), have been carried out.

The source 2FGL J0523.3−2530 is sufficiently bright that it was listed as 1FGL J0523.5−2529 in the *Fermi* LAT First Source Catalog (Abdo et al. 2010). *Swift* imaging of the field has revealed a candidate X-ray counterpart (Takeuchi et al. 2013). While radio searches for a pulsar have failed (Guillemot et al. 2012; Petrov et al. 2013), optical imaging and spectroscopy recently have discovered orbital modulations from the X-ray counterpart, with a period of 16.5 hr (Strader et al. 2014). The source is located at a high Galactic latitude $G_b = -29.^{\circ}8$ and has a late-G or early-K spectral type secondary star, and γ-ray luminosity of $\sim 3.1 \times 10^{33}$ erg s^{-1} (assuming source distance d = 1.1 kpc; Strader et al. 2014). Based on these properties, Strader et al. (2014) suggested that the source is likely a millisecond pulsar binary (MSP) with a 0.8 $M_{\odot}$ companion. Furthermore, this binary could be another so-called "redback" system, which is classified as an eclipsing MSP binary that contains a relatively massive ($\gtrsim$0.2 $M_{\odot}$), nondegenerate companion (Roberts 2013). The ablation of the companion by pulsar wind from the MSP produces matter in the binary, which would eclipse radio emission from the pulsar at certain orbital phases.

We were intrigued by this *Fermi* source because we note that it is located in the blazar region, along with the Crab pulsar, in the curvature–variability plane of *Fermi* bright sources (see Figure 4 in Romani 2012), which suggests possible variability from this source. It has recently been learned that the prototypical redback system PSR J1023+0038 (Archibald et al. 2009) has shown γ-ray variability due to its temporary accretion activity (Stappers et al. 2014; Patruno et al. 2014; Takata et al. 2014). Another newly identified redback system, XSS J12270−4859, which underwent a transition from X-ray binary to MSP binary in 2012 November–December (Roy et al. 2014; Bassa et al. 2014; Bogdanov et al. 2014), is also known to have γ-ray emission (Hill et al. 2011). Given the discovery of the orbital period of 2FGL J0523.3−2530 and its properties listed above, we have thus carried out detailed analysis of the *Fermi* data for this source, aiming to study the source's γ-ray flux variations, determine its high-energy properties, and establish the similarities to the redback systems PSR J1023+0038 and XSS J12270−4859 in particular. In addition, since there are two sets of archival *Swift* X-ray data available for the source, we also conducted X-ray data analysis. In this paper, we report the results from the analyses.

2. OBSERVATION

LAT is the main instrument on board *Fermi*. It is a γ-ray imaging instrument which performs all-sky surveys in the energy range from 20 MeV to 300 GeV (Atwood et al. 2009). In our analysis, we selected LAT events from the *Fermi* Pass 7 Reprocessed (P7REP) database inside a $20^{\circ} \times 20^{\circ}$ region centered at the catalog position of 2FGL J0523.3−2530 (Nolan et al. 2012). We kept events during the time period from 2008 August 4 15:43:36 to 2014 April 2 01:49:57 (UTC), and rejected events below 200 MeV because of the relatively large uncertainties of the instrument response function of the LAT in the low energy range. In addition we followed the recommendations of the LAT

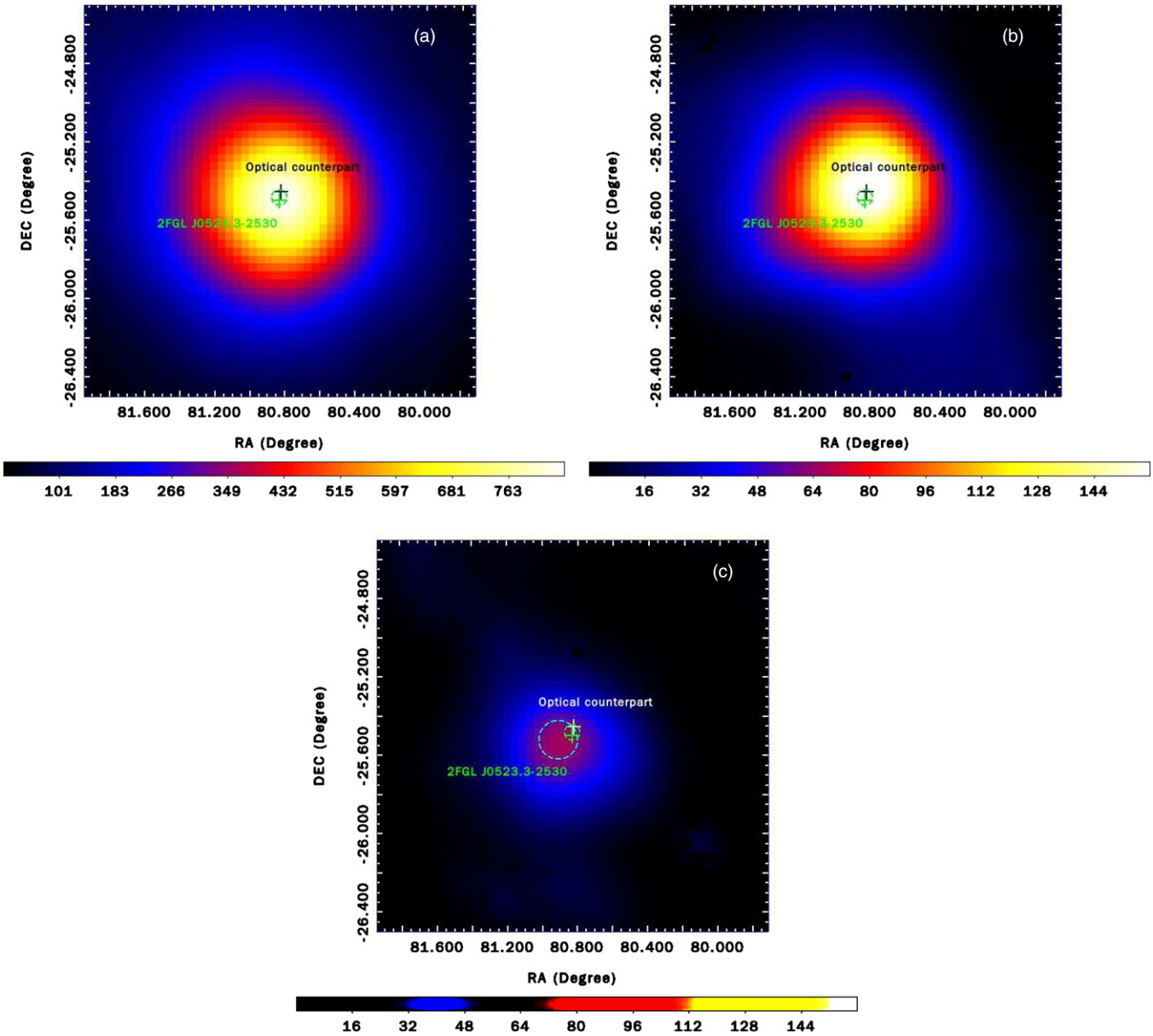

Figure 1. TS maps of a $2^{o} \times 2^{o}$ region centered at 2FGL 0523.3−2530, with all sources in the source model considered and removed. Panel (a) is a 0.2–300 GeV map made from the whole *Fermi* data. Panels (b) and (c) are 1–300 GeV maps during the time interval I and II, respectively, that are defined in Section 3.2. The green and dark (or white in panel (c)) crosses mark the catalog and optical positions, respectively, of 2FGL 0523.3−2530. The green dashed circles indicate the 2σ error circle centered at the best-fit position. The large circle in panel (c) indicates the 2σ error circle of the source during time interval II.

(A color version of this figure is available in the online journal.)

team to include only events with zenith angle less than 100°, which prevents contamination from the Earth's limb, and during good time intervals when the quality of the data was not affected by the spacecraft events.

3. DATA ANALYSIS AND RESULTS

3.1. Source Identification

We included all sources within 16° centered at the position of 2FGL J0523.3−2530 in the *Fermi* two-year catalog (Nolan et al. 2012) to make the source model. The spectral models of these sources are provided in the catalog. The spectral normalization parameters of the sources within 8 deg from 2FGL J0523.3−2530 were set free, and all the other parameters of the sources were fixed at their catalog values. We also included the Galactic and extragalactic diffuse emission in the source model, using the spectral model gll_iem_v05.fits and the spectrum file iso_source_v05.txt, respectively. The normalizations of the diffuse components were set as free parameters.

We performed standard binned likelihood analysis on the LAT >0.2 GeV data using the LAT science tools software package `v9r23p5` and extracted the Test Statistic (TS) map of a $2^{\circ} \times 2^{\circ}$ region centered at the position of 2FGL J0523.3−2530 (panel (a) of Figure 1), with all sources in the source model considered. A TS value is calculated from $\mathrm{TS} = -2\log(L_0/L_1)$, where L_0 and L_1 are the maximum likelihood values for a model without and with an additional source at a specified location, respectively, and is a measurement of the fit improvement for including the source. Generally, the TS is approximately the square of the detection significance of a source (Abdo et al. 2010). The γ-ray

Table 1
Binned Likelihood Analysis Results for 2FGL J0523.3−2530

Spectral model	Flux/10^{-9} (photon cm^{-2} s^{-1})	Γ	E_c (GeV)	TS
Power law	11.5 ± 0.7	2.17 ± 0.04	···	848
Exponentially cutoff power law	9.3 ± 0.8	1.6 ± 0.1	4.4 ± 1.0	889
Exponentially cutoff power law[a]	9.6 ± 1.0	1.8 ± 0.1	6.2 ± 2.4	452

Note. [a] The results are from analyzing the low state data (see Section 3.3).

emission near the center was detected with TS $\simeq$ 800, indicating a $\sim 28\sigma$ detection significance. We ran *gtfindsrc* in the LAT software package to find the position of the γ-ray emission in this region and obtained a position of R.A. = 80.°83, decl. = −25.°49 (equinox J2000.0), with a 1σ nominal uncertainty of 0.°02. The catalog position of 2FGL J0523.3−2530 is R.A. = 80.°83, decl. = −25.°50 (equinox J2000.0), and the position of the optical binary is R.A. = 80.°8205, decl. = −25.°4603 (equinox J2000.0, Strader et al. 2014; the uncertainty is determined by the USNO-B systematic accuracy of 0.″2, Monet et al. 2003). The optical position is ∼0.°03 from the best-fit position, but within the 2σ error circle.

The >0.2 GeV emission from 2FGL J0523.3−2530 was analyzed by modeling with a simple power law and an exponentially cutoff power law (characteristic of pulsar γ-ray emission)y. The results are given in Table 1. The source modeled with the power-law spectrum was found to have spectral index $\Gamma = -2.17 \pm 0.04$ and a TS_{pl} value of $\simeq$848, while that with the exponentially cutoff power-law spectrum has $\Gamma = -1.6 \pm 0.1$, cutoff energy $E_c = 4.4 \pm 1.0$ GeV, and a $\mathrm{TS}_{\mathrm{exp}}$ value of $\simeq$889. Therefore, the cutoff was detected with $\sim 6\sigma$ significance (estimated from $\sqrt{\mathrm{TS}_{\mathrm{exp}} - \mathrm{TS}_{pl}} = \sqrt{41}$).

3.2. Long-term Variability Analysis

To investigate the variability of 2FGL J0523.3−2530, we extracted different time-interval γ-ray light curves at different energy bands (>0.2 GeV, >1 GeV, or >2 GeV bands). The light curves were extracted by performing likelihood analysis on the LAT data in each time bin. The emission of a point source with a power-law spectrum at the best-fit position was considered for the source. The spectral index was fixed at the value given in Table 1. By comparing the obtained TS values at the source position, we found that the >1 GeV, 90 day interval light curve shows the most significant variations. In Figure 2, we display the light curve and TS curve. It is clear that the TS value varies between 10–80, while the corresponding flux shows a factor of four variation. For comparison, we also obtained the 0.2–1.0 GeV light curve and TS curve and plot them in Figure 2. The low energy TS curve generally has low values, similar to those of the >1 GeV one when the latter is in a "low" state. The flux is approximately 10^{-8} photons cm^{-2} s^{-1}, consistent with being constant within the uncertainties.

Based on the TS curve, we defined six time intervals. In interval II and IV, the TS curve is flat with values of <20, while in interval I and III, the TS curve has values of 30–80. In intervals V and VI, the TS values are mostly low but with weak variations in the range of 10–30. To confirm the variations seen in the light curves, we further extracted the >1 GeV TS maps during the six time intervals. In Figure 1, we display the TS maps of intervals I and II as examples of the source being bright and dim, respectively. The variations are real. The TS values at the source position are $\simeq$170 and $\simeq$60 in the two maps, indicating

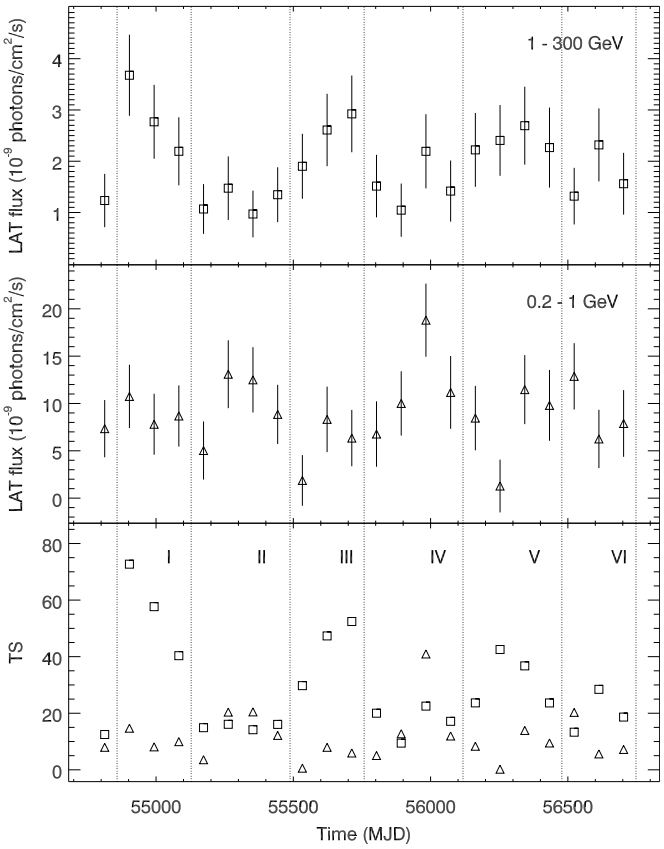

Figure 2. 90 day interval light curves and TS curves of 2FGL J0523.3−2530. The squares and triangles are the 1–300 GeV and 0.2–1.0 GeV data points, respectively. The dotted lines mark the six time intervals we defined.

approximately a 10σ significance for the flux variation between the two time intervals.

We noted that as shown in panel (c) of Figure 1 (when the source was dim), the TS peak appears to have an offset from the best-fit position. We determined the source position for time interval II and found that the position is consistent with the best-fit position within 2σ. We further checked the TS maps when the source was dim (time intervals IV, V, and VI), and the TS peaks all appear to have small offsets from the best-fit position but in different directions. In our analysis, this *Fermi* source is consistent with being a point source, and no signs of extended emission or an additional source were found. We concluded that the apparent offsets are probably due to underestimated uncertainties for the source position.

3.3. Spectral Analysis

The γ-ray spectrum of 2FGL J0523.3−2530 was extracted by performing maximum likelihood analysis on the LAT data in 15 evenly divided energy bands in logarithm from 0.1–300 GeV.

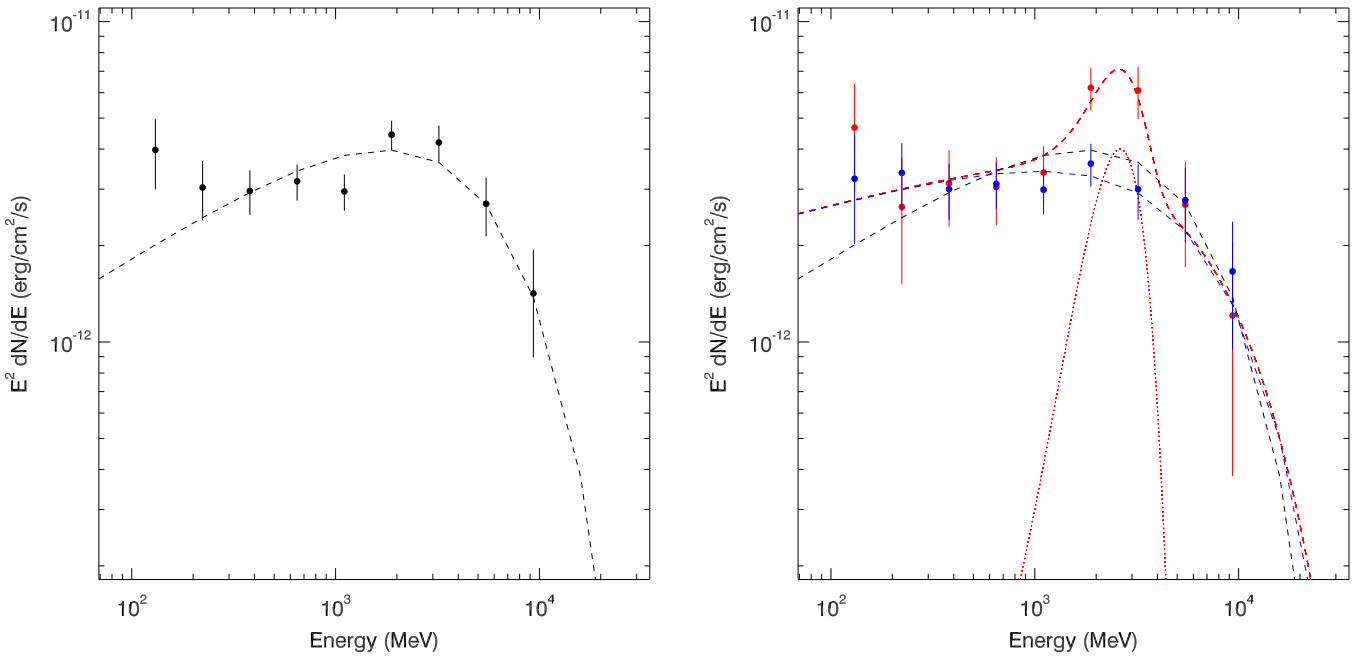

Figure 3. γ-ray spectra of 2FGL J0523.3−2530 during the whole LAT observation (left panel), and during the high (red data points) and low (blue data points) states (right panel). The exponentially cutoff power law obtained from maximum likelihood analysis for the whole data is shown as black dashed curves, and for the low state data is plotted as the blue dashed curve. A Gaussian function (red dotted curve) can be added to the spectrum to describe the extra component at 2–3 GeV.

(A color version of this figure is available in the online journal.)

Table 2
Flux Measurements for 2FGL J0523.3−2530

E (GeV)	$F_{\rm low}/10^{-12}$ (erg cm^{-2} s^{-1})	$F_{\rm high}/10^{-12}$ (erg cm^{-2} s^{-1})	$F_{\rm total}/10^{-12}$ (erg cm^{-2} s^{-1})
0.13	3.2 ± 1.2	4.7 ± 1.7	4.0 ± 1.0
0.22	3.4 ± 0.8	2.6 ± 1.1	3.0 ± 0.6
0.38	3.0 ± 0.6	3.1 ± 0.8	3.0 ± 0.5
0.65	3.1 ± 0.5	3.0 ± 0.7	3.2 ± 0.4
1.10	3.0 ± 0.5	3.4 ± 0.7	2.9 ± 0.4
1.88	3.6 ± 0.5	6.2 ± 0.9	4.4 ± 0.5
3.21	3.0 ± 0.6	6.1 ± 1.1	4.2 ± 0.5
5.48	2.8 ± 0.7	2.7 ± 1.0	2.7 ± 0.6
9.34	1.7 ± 0.7	1.2 ± 0.8	1.4 ± 0.5

Note. $F = E^2 dN/dE$, obtained from the data during the low state (Column 2) and high state (Column 3), and from the total data (Column 4).

The source was modeled with a power-law spectrum, and the spectral index was fixed at the value we obtained above (Table 1). The obtained γ-ray spectrum is shown in Figure 3 and the values at each bin are given in Table 2, in which the spectral points with TS greater than 4 were kept. The cutoff power law model is also displayed in Figure 3. The model does not describe the low-energy data points well, as two data points are approximately 2σ away from the cutoff power-law model (black dashed curve in Figure 3).

To search for differences in the source's emission during the "high" and "low" states shown in Figure 2, and thus help us understand the cause of the flux variation, we extracted γ-ray spectra of 2FGL J0523.3−2530 during the two states. We used TS = 30 to define the source's two states. The spectra obtained during the high (TS $\geqslant$ 30) and low (TS < 30) states are plotted in Figure 3. The flux values are given in Table 2. By comparing the two spectra, a component at the 2–3 GeV energy range during the high state is present. We therefore further modeled the low state emission with a cutoff power law, and found $\Gamma = 1.8 \pm 0.1$, $E_c = 6.2 \pm 2.4$ GeV. This model is displayed in the right panel of Figure 3, showing that it describes well the low-state spectrum and the high-state one when excluding the 2–3 GeV data points. A Gaussian function, $A\exp[-(E - E_0)^2/2\sigma^2]$, where $A = (4 \pm 1) \times 10^{-12}$ erg cm^{-2} s^{-1}, $E_0 = 2.6 \pm 0.2$ GeV, and $\sigma = 0.7 \pm 0.2$ GeV, may be added to the model spectrum to describe the extra component. The reduced χ^2, which is 3.2 (for six degrees of freedom) when comparing the high-state spectrum with the cutoff power law, is improved to 1.0 (for three degrees of freedom) when the Gaussian component is included.

3.4. Timing Analysis

Around the frequency $1.68195 \pm 0.00007 \times 10^{-5}$ Hz, which was determined from optical radial velocity measurements by Strader et al. (2014), orbital modulations were searched for in the γ-ray emission of the source. The search was performed on the LAT data within 1°.0 from the optical position of 2FGL J0523.3−2530, and *gtpsearch* in the LAT software package was used. The optical position was used for the barycentric correction to photon arrival times. Different energy ranges of >0.2 GeV, >1 GeV, >2 GeV, and >3 GeV were considered in our search. No significant signals were found for the whole data. We also searched in the individual time periods marked by Figure 2. No signals were detected during the high state; in the low state marginal signals were seen, but none of them were sufficiently convincing as the *H*-test values for the signals were approximately 10.

Given the uncertainty of the orbital period, we considered that in time intervals V and VI, the optical timing results are reliable (note that the binary orbit was determined from optical observations during from 2013 October 1 to 2014 January 10; Strader et al. 2014) and the source was mostly in the low state. We thus searched for periodic signals during a slightly longer time period from 2012 October 1 to the end of the LAT data we

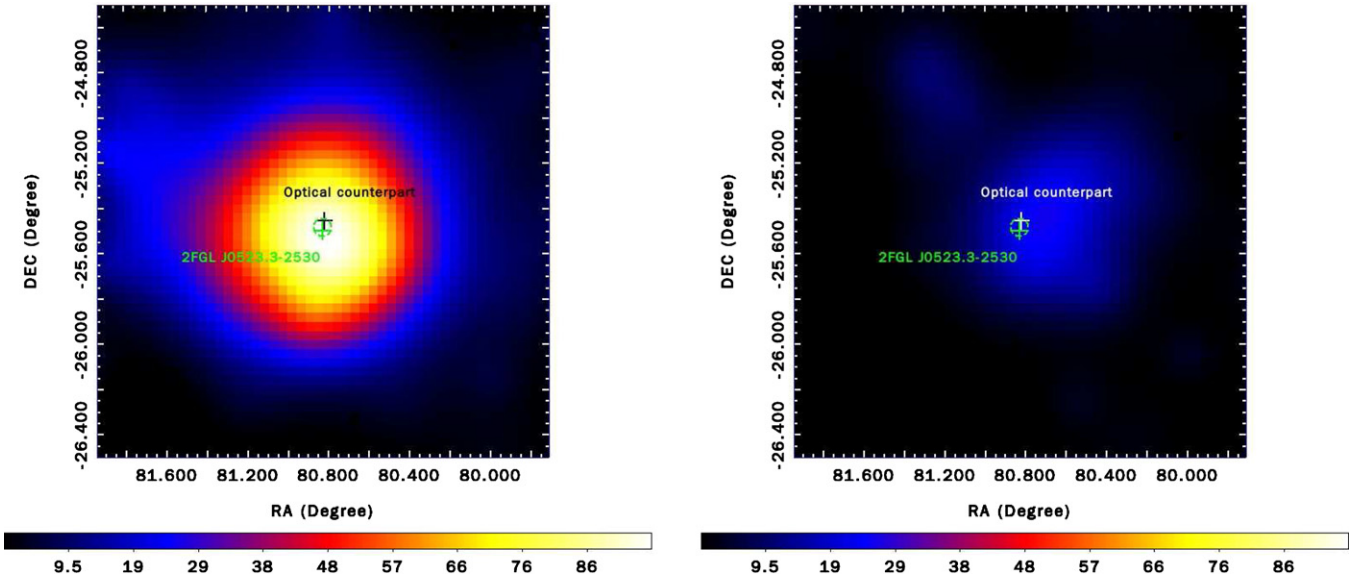

Figure 4. TS maps (2–300 GeV) of a $2^{o} \times 2^{o}$ region centered at 2FGL 0523.3−2530 during two half orbits centered at the inferior conjunction (left panel) and superior conjunction (right panel), respectively. The data are from 2012 October 1 to 2014 April 2. Symbols are the same as in Figure 1.
(A color version of this figure is available in the online journal.)

analyzed. Folding >2 GeV data at the optical period, a signal with an *H*-test value of 15 was found. Following Wu et al. (2012), we also made two TS maps over two half orbital phases to confirm the detection of the orbital flux variations. Phase I is the half of the orbit centered at the superior conjunction (when the secondary is behind the primary star), and Phase II is the other half centered at the inferior conjunction. The TS maps are shown in Figure 4. The >2 GeV γ-ray emission from 2FGL J0523.3−2530 during Phase II is more significantly detected than that during Phase I, with TS values of $\simeq$90 and $\simeq$20, respectively, at the source position.

We also searched for the periodic signals in the same energy range and over the same time period. A signal with an *H*-test value of $\simeq$18 ($\sim 4\sigma$ detection significance) at the frequency of 1.682246×10^{-5} Hz was found. This frequency is within the 5σ error range of the optical orbital value. The folded light curve is shown in Figure 5, where phase zero is set at the superior conjunction (MJD 56577.14636, given by Strader et al. 2014). The source was brighter during the phase of 0.25–0.55 (Phase II is 0.25–0.75). Spectra during the on-peak and off-peak phases were obtained, but due to the limited numbers of photons, the uncertainties on the flux data points are too large to allow any further detailed analysis.

No attempt was made to search for millisecond spin signals from the primary star, since it is difficult and computing-intensive to find from blind searches of *Fermi* γ-ray data, and thus far only one MSP has been found from blind searches (Pletsch et al. 2012). We note that to search for the spin signal from the putative MSP, the low-state time periods should be considered, since emission during that time would primarily come from the pulsar (see Section 4).

3.5. *Swift* X-ray Data Analysis

The source 2FGL J0523.3−2530 was observed with *Swift* on 2009 November 12 (ObsID: 00031535001) and on 2013 September 17 (ObsID: 00032938001) for 4.8 and 14.4 ks, respectively. We analyzed the photon counting mode data from the X-ray Telescope. The data were processed by the standard pipeline, and in both observations, an X-ray source is clearly detected at the optical position. Using a standard extraction aperture of 20 pixels (= 47.″1) radius, we obtained 14 ± 4 and 57 ± 8 background-subtracted counts for the first and second exposures, respectively, in 0.3–7 keV. These correspond to count rates of $2.9 \pm 0.9 \times 10^{-3}$ and $4.0 \pm 0.6 \times 10^{-3}$ counts s^{-1}, respectively. Given the large uncertainties, these two values are formally consistent. The source was too faint and the two observations were too short (comparing to the orbital period) to be searched for orbital modulation.

We extracted the source spectrum from the merged data set using the aperture mentioned above. The spectral analysis was carried out in XSPEC in the 0.3–7 keV energy range, using the telescope response files provided by the calibration team. For the spectral fit, we employed the *C*-statistic (cstat in XSPEC) to perform unbinned likelihood analysis due to the low number of counts. We first tried an absorbed power-law model, but found a very small absorption column density. This is not surprising since the source is at a high Galactic latitude and the total Galactic column density in the direction is only 1.7×10^{20} cm^{-2} (Kalberla et al. 2005). We therefore did not include absorption in the final fit and obtained a photon index of $\Gamma = 1.5 \pm 0.2$ with a goodness-of-fit equivalent to a reduced χ^2 value of 0.96. The energy flux is 1.3×10^{-13} erg cm^{-2} s^{-1} in 0.3–7 keV.

4. DISCUSSION

From our analysis of the *Fermi* data for 2FGL J0523.3−2530, we have found significant γ-ray flux variations over approximately 5.5 yr of *Fermi* observation time. Spectral analysis of the data during the high and low states indicates that emission from the source in the latter is well described by an exponentially cutoff power law, which is typical for pulsar emission. Comparing to the MSPs detected with *Fermi* (Abdo et al. 2013), the cutoff energy is among the highest but within the uncertainties (the highest value with smaller uncertainty is $E_c = 5.3 \pm 1.1$). If this source is an MSP binary as suggested, the emission in the low state is likely dominated by that from the pulsar (however, see discussion below). As shown in Figure 2, in the low state,

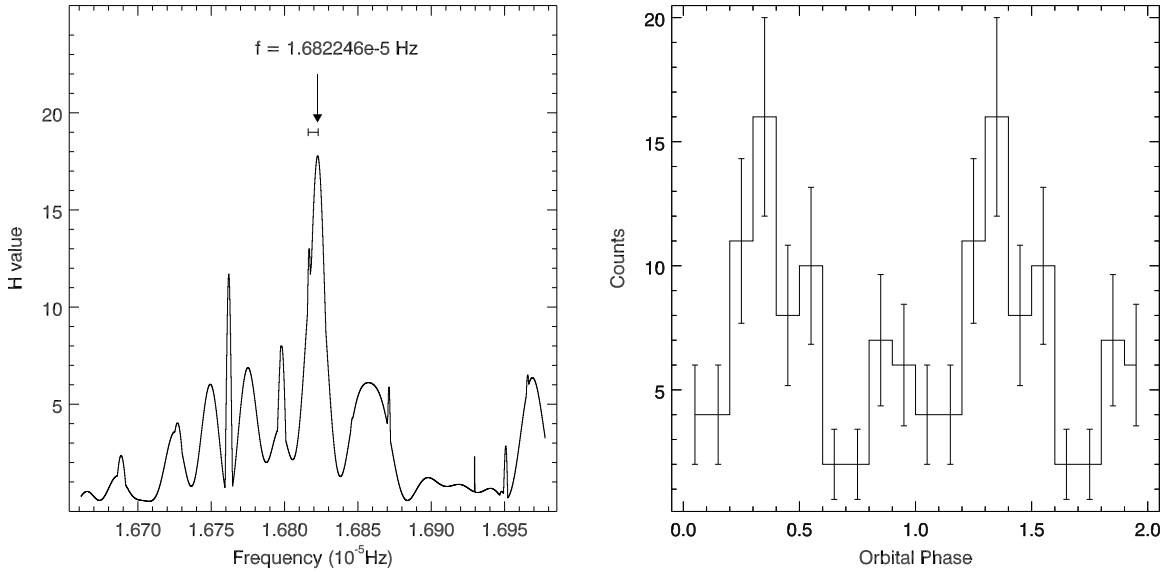

Figure 5. Left panel: *H*-test values at trial frequencies resulting from the 2012 October 1 to 2014 April 2 data. The frequency with the highest *H*-test value is marked by an arrow. The error bar indicates the 5σ error range of the optical orbital period. Right panel: folded light curve (>2 GeV energy range) at the highest *H*-test value frequency indicated in the left panel.

the TS values in the energy ranges of 0.2–1 GeV and 1–300 GeV are consistently low, not having any drastically differences as seen in the high state.

Our spectral analysis also shows that the variability mainly comes from the presence of an extra component at 2–3 GeV. We note that the flux changes could be rapid. For example, at the beginning of time interval I (Figure 2), the flux has a sudden increase by a factor of four. To investigate the jump, we also made a 10 day interval light curve; the sudden jump still exists, which suggests that the timescale for the flux change would probably be within 10 days. This timescale is reminiscent of PSR J1023+0038 in 2013 late June, when the pulsar binary was found to have an accretion disk again (Takata et al. 2014). The γ-ray flux from the pulsar binary was also 10 times larger than before, a factor of two times higher than what was seen in 2FGL J0523.3−2530. Would the flux changes be also due to the presence of an accretion disk if the source is considered as another transitional pulsar binary? The nondetection of any orbital modulation signals during the high state would support this scenario, since additional emission from the temporary disk is suggested to be the cause of γ-ray brightening seen in PSR J1023+0038 (Takata et al. 2014). However, the optical light curve of 2FGL J0523.3−2530 reported by Strader et al. (2014) does not support such a case. The light curve was from data points taken from 2005 August to 2013 April, which covers the *Fermi* observation time, but does not show any signs of irradiation of the companion or additional optical emission from a disk. We also note that the two sets of X-ray data were both taken during the low state, which may explain the consistent faintness of the source during the two X-ray observations.

We have detected orbital modulation in γ-ray emission of 2FGL J0523.3−2530, although only in the last 1.5 yr data of the total *Fermi* observation. Unfortunately, due to the limited photon counts, we were not able to obtain any spectral information about the differences between the on-peak and off-peak emission. Thus far, the prototypical black widow pulsar binary B1957+20, in which a degenerate, low-mass companion is under strong irradiation by pulsar wind from an MSP (Fruchter et al. 1988), is the only compact binary detected with orbital γ-ray modulation (Wu et al. 2012). Similarly, Phase II of this binary was found to be brighter, due to excess emission at the >2.7 GeV high energy range. The excesses have been explained to be due to inverse Compton (IC) scattering of the thermal photons from the companion by the pulsar wind (see Wu et al. 2012 for details). The same radiation mechanism has also been considered by Bednarek (2014) for modulated γ-ray emission from MSP binaries, although the detailed physical processes are different. In any case, the modulation arises due to changes of the viewing angle to the intrabinary γ-ray producing region as the binary rotates. The high cutoff energy seen in 2FGL J0523.3−2530 in the low state could be because there is a similar extra component, arising from the intrabinary interaction. The fact that orbital modulation only appears in >2 GeV emission supports this possibility. In addition, the X-ray emission had a power-law spectrum similar to that of PSR J1023+0038 (Archibald et al. 2010; Bogdanov et al. 2011) and XSS J12270−4859 (Bogdanov et al. 2014), and black widow pulsars (e.g., Gentile et al. 2014), and the *Swift* X-ray luminosity was 1.9×10^{31} erg s^{-1} (at distance 1.1 kpc), lower but comparable to that of PSR J1023+0038 and XSS J12270−4859 when these two sources are at their no-disk states. The X-ray similarity thus suggests the existence of the intrabinary interaction as well. We may even speculate that the yearly variability of 2FGL J0523.3−2530 is due to an enhanced intrabinary interaction of the pulsar wind with the companion (or outflow of the companion), resulting in the presence of the 2–3 GeV component. However, if this is the case, we would probably expect easier detection of orbital modulation when the source was in the high state, contrary to what is learned from our data analysis.

Due to the relatively large $0.^{\circ}2$ error circle of *Fermi* sources, it can be difficult to exclude any possible contamination from other sources within the error circle. For example, in the XSS J12270−4859 field, a radio-jet source and a candidate galaxy cluster have been found, which may contribute to the γ-ray emission (and possible flux variations) detected (Hill et al. 2011;

Bogdanov et al. 2014). We note that in the SIMBAD database, none of the known nearby sources in the field could possibly be associated with 2FGL J0523.3−2530, although Schinzel et al. (2014) have very recently reported the detection of a radio source 0.°037 away in their effort to search for radio sources possibly associated with *Fermi* objects. The majority of the high Galactic *Fermi* objects ($Gb \geqslant 10^{\circ}$) are associated with active galactic nuclei (AGNs; Nolan et al. 2012), and they are strong variable sources. However no evidence supports the presence of an AGN in the field. Emission from AGNs generally has a power-law form, arising due to IC scattering by high-energy electrons in jets from the AGN (Abdo et al. 2009). Their spectral features (e.g., Williamson et al. 2014) are clearly different from that seen in the high state of 2FGL J0523.3−2530: if there is an AGN causing the variability, the flux increases should have occurred over the whole energy range. Moreover, the probability of having a γ-ray emitting AGN in the field is really low. On the basis of the AGN counts distribution study in Abdo et al. (2009), the number of AGNs with *Fermi* γ-ray fluxes greater than 10^{-8} photons cm^{-2} s^{-1} is 0.064 deg^{-2}. For the 0.°06 radius (3σ) error circle region, the probability of having at least one such AGN is only 6.8×10^{-4}. Given these reasons, it is not likely that the variability is caused by the existence of an unknown AGN.

In summary, we have detected orbital modulation in the >2 GeV γ-ray emission of 2FGL J0523.3−2530, which confirms the association of this source with the optical binary. In addition, long-term, yearly variability from this γ-ray source has also been detected, and the flux increases are due to the presence of an extra emission component at 2–3 GeV. The origin of the component as well as the variability is not clear. In the near future, multiwavelength studies of the source and source field should be conducted, aiming to detect any correlated flux variations at optical/X-ray energies and help determine the origin of the high-energy component and its variability.

We thank the anonymous referee for useful suggestions and Liang Chen for helpful discussion about *Fermi* properties of AGNs.

This research was supported by the Shanghai Natural Science Foundation for Youth (13ZR1464400), the National Natural Science Foundation of China (11373055), and the Strategic Priority Research Program "The Emergence of Cosmological Structures" of the Chinese Academy of Sciences (grant No. XDB09000000). Z.W. is a Research Fellow of the One Hundred Talents project of the Chinese Academy of Sciences.

REFERENCES

Abdo, A. A., Ackermann, M., Ajello, M., et al. 2009, ApJ, 700, 597
Abdo, A. A., Ackermann, M., Ajello, M., et al. 2010, ApJS, 188, 405
Abdo, A. A., Ajello, M., Allafort, A., et al. 2013, ApJS, 208, 17
Acero, F., Donato, D., Ojha, R., et al. 2013, ApJ, 779, 133
Ackermann, M., Ajello, M., Allafort, A., et al. 2012, ApJ, 753, 83
Archibald, A. M., Kaspi, V. M., Bogdanov, S., et al. 2010, ApJ, 722, 88
Archibald, A. M., Stairs, I. H., Ransom, S. M., et al. 2009, Sci, 324, 1411
Atwood, W. B., Abdo, A. A., Ackermann, M., et al. 2009, ApJ, 697, 1071
Bassa, C. G., Patruno, A., Hessels, J. W. T., et al. 2014, MNRAS, 441, 1825
Bednarek, W. 2014, A&A, 561, A116
Bogdanov, S., Archibald, A. M., Hessels, J. W. T., et al. 2011, ApJ, 742, 97
Bogdanov, S., Patruno, A., Archibald, A. M., et al. 2014, ApJ, 789, 40
Fruchter, A. S., Stinebring, D. R., & Taylor, J. H. 1988, Natur, 333, 237
Gentile, P. A., Roberts, M. S. E., McLaughlin, M. A., et al. 2014, ApJ, 783, 69
Guillemot, L., Freire, P. C. C., Cognard, I., et al. 2012, MNRAS, 422, 1294
Hill, A. B., Szostek, A., Corbel, S., et al. 2011, MNRAS, 415, 235
Kalberla, P. M. W., Burton, W. B., Hartmann, D., et al. 2005, A&A, 440, 775
Monet, D. G., Levine, S. E., Canzian, B., et al. 2003, AJ, 125, 984
Nolan, P. L., Abdo, A. A., Ackermann, M., et al. 2012, ApJS, 199, 31
Patruno, A., Archibald, A. M., Hessels, J. W. T., et al. 2014, ApJL, 781, L3
Petrov, L., Mahony, E. K., Edwards, P. G., et al. 2013, MNRAS, 432, 1294
Pletsch, H. J., Guillemot, L., Fehrmann, H., et al. 2012, Sci, 338, 1314
Ray, P. S., et al. 2012, arXiv:1205.3089
Roberts, M. S. E. 2013, in IAU Symp. 291, Neutron Stars and Pulsars: Challenges and Opportunities after 80 years, ed. J. van Leeuwen (Cambridge: Cambridge Univ. Press), 127
Romani, R. W. 2012, ApJL, 754, L25
Roy, J., Bhattacharyya, B., & Ray, P. S. 2014, ATel, 5890, 1
Schinzel, F. K., Petrov, L., Taylor, G. B., et al. 2014, arXiv:1408.6217
Stappers, B. W., Archibald, A. M., Hessels, J. W. T., et al. 2014, ApJ, 790, 39
Strader, J., Chomiuk, L., Sonbas, E., et al. 2014, ApJL, 788, L27
Takata, J., Li, K. L., Leung, G, C. K., et al. 2014, ApJ, 785, 131
Takeuchi, Y., Kataoka, J., Maeda, K., et al. 2013, ApJS, 208, 25
Williamson, K. E., Jorstad, S. G., Marscher, A. P., et al. 2014, ApJ, 789, 135
Wu, E. M. H., Takata, J., Cheng, K. S., et al. 2012, ApJ, 761, 181